Earth's Future

RESEARCH ARTICLE
10.1029/2023EF003556

Special Section:
CMIP6: Trends, Interactions, Evaluation, and Impacts

Intensification of Extreme Rainfall in Indian River Basin: Using Bias Corrected CMIP6 Climate Data

Pawan K. Chaubey[1] and **Rajesh K. Mall**[1]

[1]DST-Mahamana Centre of Excellence in Climate Change Research, Institute of Environment and Sustainable Development, Banaras Hindu University, Varanasi, India

Key Points:

- Extreme rainfall is projected to intensify in future but decrease in areal mean rainfall in near and far future
- Central and west Indian river basins will be more vulnerable
- The finding support flood and emergency policies to mitigate the extreme rainfall impacts

Supporting Information:

Supporting Information may be found in the online version of this article.

Correspondence to:

R. K. Mall,
rkmall@bhu.ac.in

Citation:

Chaubey, P. K., & Mall, R. K. (2023). Intensification of extreme rainfall in Indian river basin: Using bias corrected CMIP6 climate data. *Earth's Future*, *11*, e2023EF003556. https://doi.org/10.1029/2023EF003556

Received 1 FEB 2023
Accepted 8 AUG 2023

Author Contributions:

Conceptualization: Rajesh K. Mall
Data curation: Pawan K. Chaubey
Formal analysis: Pawan K. Chaubey
Funding acquisition: Rajesh K. Mall
Investigation: Pawan K. Chaubey, Rajesh K. Mall
Methodology: Pawan K. Chaubey, Rajesh K. Mall
Project Administration: Rajesh K. Mall
Resources: Rajesh K. Mall
Software: Pawan K. Chaubey
Supervision: Rajesh K. Mall
Validation: Pawan K. Chaubey

Abstract The changing frequency of extreme rain events in the past few decades over the Indian river basins (IRBs) contributed to floods and drought and resulted in economic losses and gross domestic product. In this study, we evaluated the performance of 12 Global Circulation Models from the Coupled Model Intercomparison Project Phase 6- experiment with India Meteorological Department observed data sets to reproduce the extreme rainfall events as well as project the changes in frequency and intensity of the hydroclimate extremes in future. We found that under low emission scenarios (SSP1-2.6), the frequency of extreme rainfall is going to increase over the western ghat and northeast IRBs, while an increase in heavy rainfall intensity (14.3%) noticed under SSP2-4.5 in the upper Ganga and Indus basin. Also, approximately 4%–10% of the heavy rainfall is projected to increase over the western part of IRBs during the Near (2021–2040) and Mid (2041–2060) future. The study explored the new hotspot regions for future urban flooding due to increasing pattern of heavy rainfall in future. Moreover, the lower Ganga basin will experience agricultural drought in near future due to decreasing areal mean rainfall, which needs to be seen by policymakers for managing the excess (less) water. Also, India's northern, central, and western river basins may experience more extremes under high-emission (SSP5-8.5) scenarios that indicate challenges to mitigation. The findings of this study highlight the importance of developing long-term adaptation and mitigation strategies aimed at reducing hydroclimate vulnerability. It emphasizes the need to implement measures that enhance resilience and minimize risks associated with hydroclimate extremes at the basin level.

Plain Language Summary Global warming increases the risk of hydro-climate extremes such as floods and droughts worldwide. The increasing rate of atmospheric heat increases the water content, which is the leading cause of extreme events. The widespread variability in extreme events has affected man-made and natural systems. The study shows the changes in the extreme precipitation events under low to high-emission scenarios of the CMIP6 climate model. The uncertainty in the different climate models is reduced in this study by applying performance tests using linear and quantile bias correction approaches. The ensemble model approach is used to examine the projected changes in extreme rainfall over the different Indian river basins (IRBs). The results show changes in the frequency of heavy rainfall will be more reign over the IRBs. In addition, this research also identified the major hotspot of highly populated cities that come under different river basins for urban flooding, which help the policymaker design appropriate adaptation and mitigation strategies.

1. Introduction

Global warming has increased rapidly since the mid-20th-century due to enhancement of greenhouse gas emissions owing to more frequent and intense extreme climatic events resulting in more hydrometeorological hazards conditions (Fan et al., 2021; Giorgi et al., 2018; IPCC, 2021; Mall et al., 2019). According to the World Meteorological Organization (WMO) hydroclimatic extremes are the reason for more than 90% of worldwide catastrophes and 43% of floods (WMO, 2017). Greenhouse Gas Emissions (GHG) driven climate change will increase precipitation frequencies over the South-Asia region, including central India, in the near and far future (Rai et al., 2019; Roy & Balling, 2004). India is listed as one of the top 10 countries that experienced almost 19 disasters due to floods and had about 1282 mortality with 3.1 billion in economic losses during the year 2021 (CRED, 2021). Accordingly, estimating appropriate future climate extremes change is necessary to know how it may influence hydrology in the South-Asia region.

Visualization: Pawan K. Chaubey
Writing – original draft: Pawan K. Chaubey
Writing – review & editing: Rajesh K. Mall

According to the Intergovernmental Panel on Climate Change's (IPCC) sixth assessment report (AR6), anthropogenic activities would cause an increase in the average global surface temperature of 0.8°C–1.3°C (IPCC, 2021). The frequency of extreme precipitation events will also increase in the late 21st century due to anthropogenic warming (Mukherjee et al., 2018). End of the 21st century, the world's temperature is projected to rise by 5.7°C, making the atmosphere more volatile and hotter (Wu et al., 2022). Many research studies showed that an increasing global mean temperature reveals an increasing trend in seasonal monsoonal rainfall over South Asia (Loo et al., 2015; Mall et al., 2021). Hydroclimatic Extremes comprise extreme precipitation, drought, and flash floods, which pose a grave threat to man-made ecosystems, agriculture, humans, and natural systems (Giorgi et al., 2018; Maurya et al., 2021; Sonkar et al., 2020). Previous researchers used the Global circulation models (GCMs) data sets to analyze the future changes in hydroclimate extremes like flood and drought (Gusain et al., 2020; Krishnan et al., 2020). The new Shared Socioeconomic Pathways (SSPs) scenarios are related to the development factors such as socio-economic, sustainability, regional rivalry, inequality, fossil-fueled, and middle-of-the-road due to climate change, which help a combined analysis of vulnerabilities, adaptation, and mitigation (Riahi et al., 2017; Wu et al., 2022).

The spatiotemporal changes in hydro-climate extremes are determined by the frequency and intensity of the daily precipitation events (Salehie et al., 2023; Sarkar & Maity, 2022). According to Huang et al. (2021), due to climate change, there will be a risk of extreme precipitation over almost 46% part of the world. Due to intense precipitation, these extreme events lead to flood risk, and less precipitation leads to drought in affected area respectively (Guhathakurta et al., 2011; Mittal et al., 2014). Moreover, the continuous precipitation and temperature changes cause frequent floods in South Asia and ultimately affect food security (Douglas, 2009). India is one of the world's most vulnerable countries to hydro-climatic extremes, such as droughts and floods, which affect the Agricultural production of the nation (Anand & Oinam, 2020; Bothale & Katpatal, 2016; Gupta & Jain, 2018). Agricultural is the primary income source of India, and it precipitated about 17% of the nation's gross domestic product (GDP), but in the last few decades, a significant reduction in GDP has been observed due to agricultural drought (Chaubey et al., 2022; Gadgil & Gadgil, 2006; Konda & Vissa, 2022).

At the end of the twenty-first century, Indian river basins (IRBs) will have a warmer and wetter climate that will result in variability in the hydro-climate extremes, especially during the monsoon season over the Indian Sub-continent (Kannan & Ghosh, 2013; Kaushik et al., 2020; Mishra & Lilhare, 2016; Roxy et al., 2017). Earlier studies found an increasing trend of precipitation extremes over IRBs (Chaubey et al., 2022; Goswami et al., 2006). And these increasing extremes will cause economic losses due to damages to crops, houses, and public utilities, approximately 415 thousand crores due to floods and heavy rains over IRBs from 1951 to 2019 (CWC, 2021). Moreover, it is found that the frequency of wet days keeps increasing over peninsular India while the trend is observed to be declining over central and North India (Guhathakurta et al., 2011; Roy & Balling, 2004). Indeed, the topography, uneven population growth, and urbanization have been heavily contributing to increasing the extreme rainfall events over IRB (Chaubey et al., 2022; Mall et al., 2006). And this increasing trend of precipitation extremes needs more research on adaptation and mitigation to decrease long-term climate change vulnerability (Mall et al., 2017). The previous researcher concluded that the frequency and intensity of the precipitation extremes are projected to increase in India in the 21st century under different SSPs scenarios (Gupta et al., 2020). Moreover, the shifting of subtropical westerly jet toward the Indian continental enhances the extremity of precipitation over southern India in the future (Tiwari et al., 2023). The projected spatial extent of precipitation extremity is determined to increase in large parts of India and about 60%, with a robust increase frequency of extreme events in central India (Shahi et al., 2023). Moreover, the projected frequency is more the western Ghats and the northeast part of India, while the intensity of extreme precipitation is projected to increase in the northwest and peninsular India (Sarkar & Maity, 2022). Also, Lutz et al. (2014) resulted that the frequency of floods and their associated risk is projected to increase all over IRBs and mainly for Indus-Ganges-Brahmaputra river basins in the future warming climate.

This study used the most recent Earth system models (ESMs) and extensive climate model experiments from the sixth phase of Coupled Model Intercomparison Project (CMIP) to examine the changes in extremes. The projected extremes of GCMs data sets show high uncertainty in extreme precipitation and are associated with projected emission scenarios, regional climate variability, model parametrization schemes, internal models physics, etc (John et al., 2022; Latif, 2011). To reduce the above uncertainties, a different bias correction method is applied by researchers, in which mean-based bias correction is found to be more suitable for climate scenarios (Jaiswal et al., 2022; Saha & Sateesh, 2022; Shrestha et al., 2020; Xu et al., 2021). To illustrate the hydroclimate extremes during near, mid, and far future, the study used the indices developed by the Expert Team on Climate Change Detection and Indices (ETCCDI) used by the previous researcher (Chaubey et al., 2022; Sarkar & Maity, 2022).

Table 1
List of CMIP6 Models Used in This Study Along With Horizontal Resolution and Country of the Modeling Group

S.No.	Models	Institution/Country	Actual resolution	Resolution after regridding
1.	ACCESS-ESM1-5	Commonwealth scientific and industrial research organization/Australia	1.25° × 1.25°	1.0° × 1.0°
2.	ACCESS-CM2			
3.	BCC-CSM2-MR	Beijing Climate Center (BCC) China Meteorological Administration/China	1.125° × 1.125°	1.0° × 1.0°
4.	CMCC-ESM2	Euro-Mediterranean Center on Climate Change coupled climate model/Italy	0.9° × 1.25°	1.0° × 1.0°
5.	FGOALS-g3	Chinese Academy of Sciences (CAS)/China	2.25° × 2.0°	1.0° × 1.0°
6.	MIROC6	Model for Interdisciplinary Research on Climate (MIROC)/Japan	2.32° × 1.16°	1.0° × 1.0°
7.	MPI-ESM-1-2-LR	Max Plank Institute for Meteorology/Germany	1.875° × 1.875°	1.0° × 1.0°
8.	MPI-ESM-1-2-HR		0.9375° × 0.9375°	1.0° × 1.0°
9.	MRI-ESM2-0	Meteorological Research Institute (MRI)/Japan	1.125° × 1.125°	1.0° × 1.0°
10.	NorESM2-MM	Norwegian Climate Center/Norway	0.9375° × 1.25°	1.0° × 1.0°
11.	NorESM2-LM		1.875° × 2.5°	1.0° × 1.0°
12.	TaiESM1	Taiwan Earth System Model/Taiwan	0.9° × 1.25°	1.0° × 1.0°

The other indices, the Standardized Precipitation Index (SPI), are applied in earlier studies to examine the long-term dryness and wetness situation (McKee, 1993). This aims to analyze (a) Spatial changes in precipitation in the future, (b) Identify the hotspot regions due to the intensity and frequency of the extremes, and (c) Uncertainty in extremes due to different SSPs scenarios.

Research is structured as the data sets and methodology used in this study are introduced in Section 2. Section 3 examines the changes in precipitation extremes over the IRBs. And finally, Section 4 concludes this research.

2. Data and Methods

2.1. Observed and Projected Data Sets

The research was performed over the 22 major IRBs. This research is in the continuation of the previous research done by Chaubey et al. (2022), and the details of the 22 major IRBs are described in Figure S1 and Table S1 in Supporting Information S1. To decipher the changes in extreme precipitation, we have used observed gridded rainfall data sets taken from the India meteorological department (IMD). The analysis has been performed on the daily observed data sets at a spatial resolution of 0.25° × 0.25° (Pai et al., 2014) downloaded from the National Climate Center (NCC) of IMD. The temporal frame of the observed data sets is taken from 1951 to 2021 over the IRBs. This high-resolution daily gridded data set is created from 6955 rain gauge stations across the IRBs.

The projected analysis of precipitation amount, frequency, and intensity of the precipitation extremes are carried by simulated daily precipitation (2021–2100) following four SSPs, which are SSP1-2.6, SSP2-4.5, SSP3-7.0, and SSP5-8.5. The simulated precipitation outputs were obtained from Coupled Model Intercomparison Project-6 (CMIP6) (URL: https://esgf-node.llnl.gov/search/cmip6/). All 12 models of CMIP6 have been downloaded at the variant label r1i1p1f1 as an initial condition (Table 1). Based on energy, land use, and emission, the SSPs scenarios developed by the community of climate change researchers for an integrated study of projected climate impacts, vulnerability, adaptation, and mitigation (Riahi et al., 2017). In this study, we used a multi-model approach to estimate the future changes in hydroclimate extremes over the IRBs. Many previous researchers have used the multi-model ensemble mean approach to finding the projected precipitation extremes and showed that this is the more robust analysis to estimate extreme events (Sarkar & Maity, 2022). To examine the changes in hydroclimate extremes over the IRBs, we divided the data sets into three-time frames from 2021 to 2040 for Near-future, 2041 to 2060 for Mid-future, and 2081 to 2100 for Far-future. All the data sets have been regridded in the same spatial resolution (1° × 1°) over the IRBs, listed in Table 1.

2.2. Bias-Correction

Linear Scaling (LS) is based on a multiplicative term for rainfall bias correction, where the differences between the monthly mean of model bias corrected value and that of observation are minimized (Lenderink et al., 2007).

By definition, after applying the LS on uncorrected data, it perfectly matches the monthly mean rainfall value with the observed rainfall value. The first step involved in the method LS is calculated the monthly scaling factor as the ratio of the long-term monthly mean of observed data and model data (for the same time period selected in observed). In the second step, the scaling factor is multiplied by each of the daily values of uncorrected data for the corresponding month.

$$Pd_{\mathrm{bc(hist)}} = Pd_{\mathrm{mod}} \frac{[\mu_m(Pd_{\mathrm{obs}})]}{[\mu_m(Pd_{\mathrm{mod}})]} \tag{1}$$

$$Pd_{\mathrm{bc(proj)}} = Pd_{\mathrm{scen}} \frac{[\mu_m(Pd_{\mathrm{obs}})]}{[\mu_m(Pd_{\mathrm{mod}})]} \tag{2}$$

Where $Pd_{\mathrm{bc(hist)}}$ and $Pd_{\mathrm{bc(proj)}}$ is daily bias-corrected data for historical and projected time periods, respectively, and $\mu_m(Pd_{\mathrm{obs}})$ is the long-term monthly mean of observed rainfall. While $\mu_m(Pd_{\mathrm{mod}})$ is the long-term mean of the uncorrected model (for the historical time period) rainfall data and Pd_{scen} represents the long-term mean of the uncorrected simulated outputs (for the projected time period) of different climate scenarios.

Schmidli et al. (2006) introduced the Local intensity scaling (LOCI) method, which extends the LS method. The number of precipitation events for control and scenario run is corrected by applying the calibrated precipitation threshold (Pth, historical) using Equations 3 and 4, respectively

$$P^{*1}_{\mathrm{bc(hist)}}(d) = \begin{cases} 0, & \text{if } P_{\mathrm{(hist)}}(d) < P_{\mathrm{th,hist}} \\ P_{\mathrm{(hist)}}(d), & \text{otherwise} \end{cases} \tag{3}$$

$$P^{*1}_{\mathrm{bc(proj)}}(d) = \begin{cases} 0, & if\ P_{\mathrm{(scen)}}(d) < P_{\mathrm{th,hist}} \\ P_{\mathrm{(scen)}}(d), & \text{otherwise} \end{cases} \tag{4}$$

The scaling factor is estimated based on long-term monthly mean to confirm that the mean of corrected precipitation is equal to observed data

$$S = \frac{\mu_m\{P_{\mathrm{(obs)}}(d) \mid P_{\mathrm{(obs)}}(d) > 0\,\mathrm{mm}\}}{\mu_m\{P_{\mathrm{(mod)}}(d) \mid P_{\mathrm{(mod)}}(d) > P_{\mathrm{th,\,mod}}\} - P_{\mathrm{th,(mod)}}} \tag{5}$$

Finally, bias correction for historical and projected scenarios are:

$$P^{*}_{\mathrm{bc(proj)}}(d) = P^{*1}_{\mathrm{bc(proj)}}(d) * S \tag{6}$$

$$P^{*}_{\mathrm{bc(hist)}}(d) = P^{*1}_{\mathrm{bc(hist)}}(d) * S \tag{7}$$

Here, th = threshold and P*1 = intermediate step in bias correction.

Amongst the available bias correction methods, from simple Linear Scaling (LS) to sophisticated Empirical quantile mapping (EQM), the LS method has been used. The LS and advanced EQM has performed equally well for most of the region, but the EQM corrupts the relative trend in precipitation extremes compared to the LS. The statement is also supported by the study by Cannon et al. (2015), which mentioned that the Quantile mapping could artificially corrupt the model projection trend.

According to the model agreement (IPCC, 2021), the MMM is defined as the mean changes that provide an average estimate for the forced model climate response to a specific forcing. It is uncertain that the model consistently projects insignificant changes or significant increases and decreases during the projection period. Numerous methods have been suggested (IPCC, 2021) to differentiate significant inconsistent signals, display model robustness, and put a climate change signal into the context of internal variability. The advanced approach proposed by IPCC, taking into account the sign and significance of the change, in three distinct categories that are, First, the areas with significant change (high model agreement), Second the areas with no change (no robust change), and the third one is the areas with significant change but low agreement. In this study area, the climate models

Table 2
Definitions of ETCCDI Indices

ETCCDI indices name	Indices	Unit	Definition
Consecutive Drys days	CDD	Days	Maximum length of dry spell, maximum number of consecutive days with RR < 1 mm
Consecutive Wet days	CWD	Days	Maximum length of wet spell, maximum number of consecutive days with RR ≥ 1 mm
Contribution from heavy wet days	R90pTOT	%	Annual total rainfall when daily wet day amount >90th percentile (%); 95th percentile (%) (100*r95p/PRCPTOT)
Contribution from very heavy wet days	R95pTOT		
Max 5-day PR	Rx5day	mm	Annual max consecutive 5-day rainfall
Number of 5-day PR	R5day	days	Maximum 5-day PR total

Note. Here, PR = precipitation.

ACCESS-CM2, ACCESS-ESM, BCC-ESM1, FGOALS-g3, MPI-ESM1-2-HR, MRI-ESM2, NorESM2-LM, and NorESM2-MM are showing the same trend and can be considered as the models with the high agreement as well as no robust change. However, CMCC-ESM2, MIROC6, MPI-ESM1-2-LR, and TaiEM2 are with low agreement.

2.3. Estimation of Precipitation Extremes

To illustrate the changes in extreme precipitation over the IRBs, we have applied the extreme precipitation indices in low to high-emission scenarios. The bias-corrected CMIP6 data sets are used to calculate the precipitation extreme after applying the multi-model ensemble (MME) approach (Wang et al., 2022; Wu et al., 2022). To estimate the changes in hydro-climate extremes, we used the Expert Team on Climate Change Detection and Indices (ETCCDI), demonstrated in Table 2. In this research, the intensity and the frequency of the hydroclimate extremes events are computed by indices included under ETCCDI in warmer futures, detailed on the website (http://etccdi.pacificclimate.org/indices.shtml). To analyze the future changing climatology and precipitation extremes, we mainly used climate indices, such as Consecutive dry days (CDD), Consecutive wet days (CWD), and maximum consecutive 5-day precipitation (rx5day), which can be appropriate for agriculture stress and flood risk over the IRBs.

Moreover, to estimate the drought over the IRBs, we have used a standardized precipitation index (SPI). The SPI is characterized to estimate the intensity scale from dry to wet events as positive (surplus) to negative (deficit) index values, respectively. The drought events for any region are predictable by the index value under −1.0 for a period (McKee, 1993). We have examined the drought events in this study by fitting a gamma distribution to grid-level monthly rainfall values. Despite that, the spatial changes in drought events are calculated on a 3-month time scale for the near, mid, and far future. According to Mckee et al. (1993), the SPI classification is presented in Table 3, and the fitted gamma distribution to monthly rainfall is shown in Equation 8 below;

$$\mathrm{SPI} = (R - R_{\mathrm{mean}})/\sigma R \tag{8}$$

Where, R denotes precipitation and σ indicates standardized deviation.

The Percentage change of precipitation is computed from Equation 9. The changes in precipitation over the IRBs in the 21st century performed according to IPCC 2021 is for the Near-, Mid-, and Far-future relative to 1981–2014.

$$\%\ \text{change} = [(\text{Particular year} - \text{long term average})/\text{long term average}] * 100 \tag{9}$$

The Generalized extreme value (GEV) distribution is utilized to examine the projected return level of precipitation extremes over the IRBs. To compute the projected intensity of 10% precipitation extremes events, we estimated the 10-year return level based on annual maxima precipitation (Chaubey et al., 2022; Mannshardt-Shamseld et al., 2012). That represents the projected 10% probability of at least one precipitation extreme event in any projected year. More detailed for GEV in Chaubey et al. (2022).

Table 3
SPI Classification Applied in This Study

S.No.	SPI McKee et al. (1993)	Description
1.	≥2.00	Extremely wet
2.	1.50 to 1.99	Very wet
3.	1.00 to 1.49	Moderately wet
4.	0.50 to 0.99	Slightly wet
5.	−0.49 to 0.49	Near normal
6.	−0.99 to −0.50	Slightly dry
7.	−1.49 to −1.00	Moderately dry
8.	−1.99 to −1.50	Very dry
9.	≤ −2.00	Extremely dry

10.1029/2023EF003556

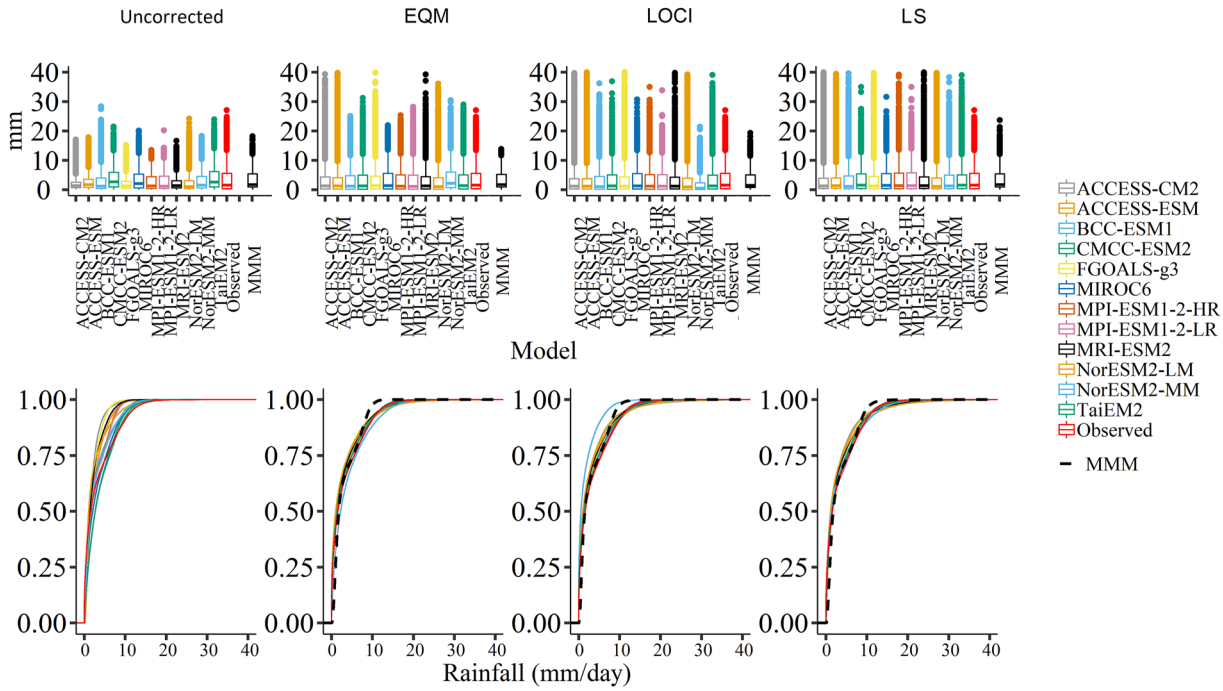

Figure 1. Bias correction validation using Boxplot and probability density distribution of precipitation from observation to 12 GCM (CMIP6) model using three bias correction methods over India.

3. Results and Discussion

3.1. Remove Biases From CMIP6 Data

To analyze the best bias correction methods for 12 CMIP6 models, we have applied a cumulative distribution function (CDF), boxplot, and Taylor diagram of both uncorrected and bias-corrected model outputs (Figure 1; Figure S2 in Supporting Information S1). The CDF of rainfall variable for uncorrected models output against IMD rainfall shows that most models have sparse distribution and the low precipitation values than observed (Figure 1). After bias correction, the best CDF matching has been estimated for the LS and EQM. In contrast, the LOCI method shows satisfactory results for all CMIP6 models except BCC-ESM1which found to be relatively far from the observed probability. In the boxplots (Figure 1), raw model output data is under predicting rainfall extremes, which improved after bias correction under each method. In the EQM, all model has shown improvements in rainfall extreme, excluding BCC-ESM1, MIROC6, MPI-ESM1-2-LR, and MPI-ESM1-2-HR, which remains under-predicted for extremes after bias correction. At the same time, the scaling method shows good agreement with extreme precipitation with slightly higher rainfall values. Therefore, all bias correction techniques have improved the rainfall variables, but scaling turns out to be the best for extreme rainfall studies in comparison with EQM and LOCI methods (Cannon et al., 2015). The statistical pattern of raw and bias-corrected data with respect to daily observed rainfall data. The majority of the uncorrected model rainfall data have correlation coefficients (CC) between 0.65 and 0.75. The Root Mean Square Error (RMSE) for raw model outputs is likewise aggregated around 3.0 to 3.5, but the Standard Deviation (SD) of various models has a more extended range from 2.0 to 3.5 (Figure S3 in Supporting Information S1). It has been estimated that the Multi-Model Mean (MMM), that is, the mean of the best 12 models, has a good correlation (0.85) with the observed IMD data sets (Figure S3 in Supporting Information S1).

The spatial pattern means precipitation MMM and IMD is shown in Figure 2. The uncorrected MMM has high uncertainty with the bias of −3 to 7 mm/day mean precipitation. However, after bias correction, we found that MMM over the has low uncertainty in precipitation with a bias of −0.3 to 0.9 mm/day. The uncorrected MMM was underestimated to some extent, with the IMD likely over the northeast river basins, whereas west-flowing river basins Tapti to and Tadri to Kanyakumari, have overestimated slightly with bias +5 to +7 mm/day. Thus MMM makes statistical analysis more feasible and suggests MMM as an optimistic approach to examining future

10.1029/2023EF003556

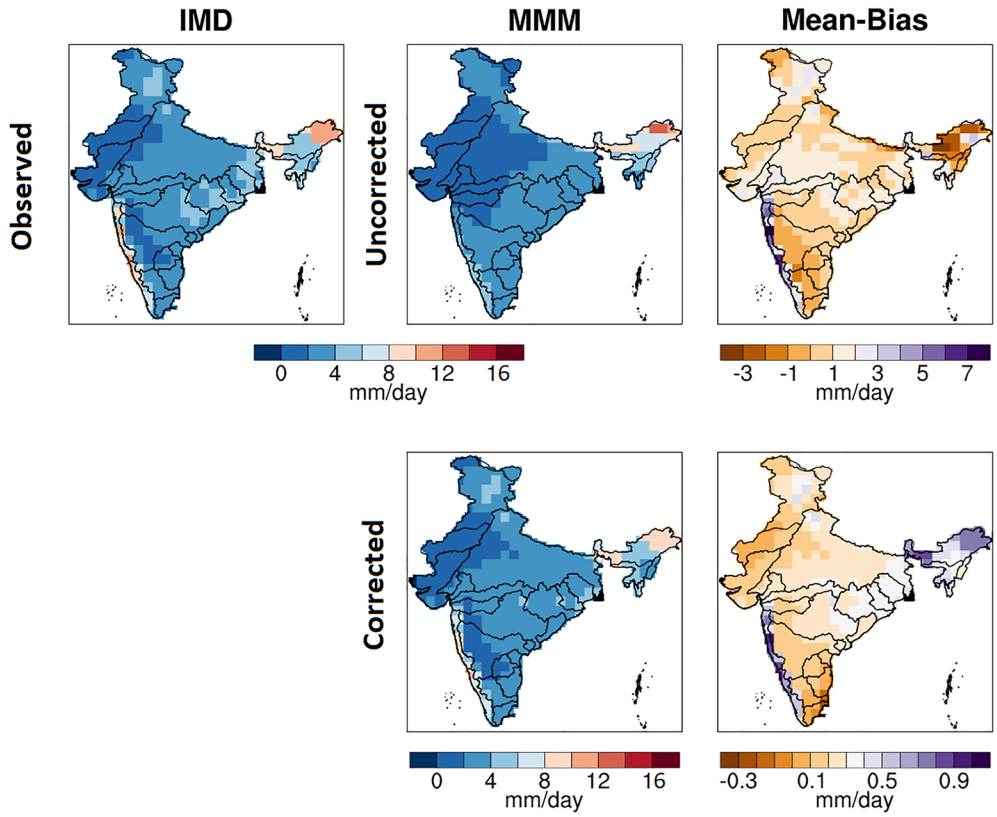

Figure 2. Spatial pattern of observed rainfall from IMD and Multi-modal Mean (MMM) of simulated outputs CMIP6 and its mean bias for uncorrected and corrected CMIP6 data sets from 1951 to 2014.

extremes with less uncertainty. Previous research (katzenberger et al., 2021) used the MMM of CMIP6 and concluded an increasing trend in rainfall over the Indian continent in the higher-warming scenarios. Trenberth et al. (2003) concluded that the regions with higher mean rainfall, there is generally a greater potential for extreme rainfall events to occur. This is because areas with higher mean rainfall often have conditions conducive to the formation of intense convective storms or persistent rainfall systems.

3.2. Spatial Changes in Precipitation Over IRBs

The spatial changes in precipitation over the IRBs show very intense variation in precipitation. Figure 3 shows the mean precipitation climatology from 2021 to 2100 over the different SSPs scenarios. We found that the areal mean precipitation is gradually increased with increasing low to high-emission scenarios. The average areal mean precipitation increases from low (38.22 mm/day) to high (39.82 mm/day) with 4.08% changes in daily mean

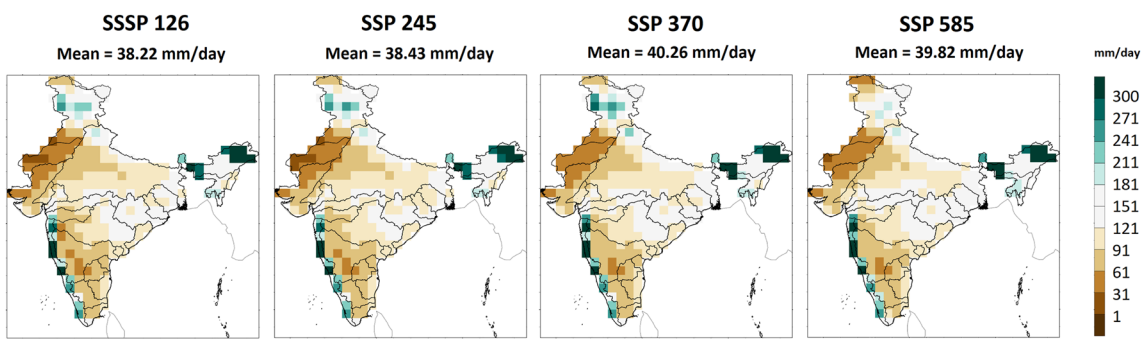

Figure 3. Climatological projected areal mean precipitation (mm/day) for 86 years over the different IRBs in all SSPs scenarios.

10.1029/2023EF003556

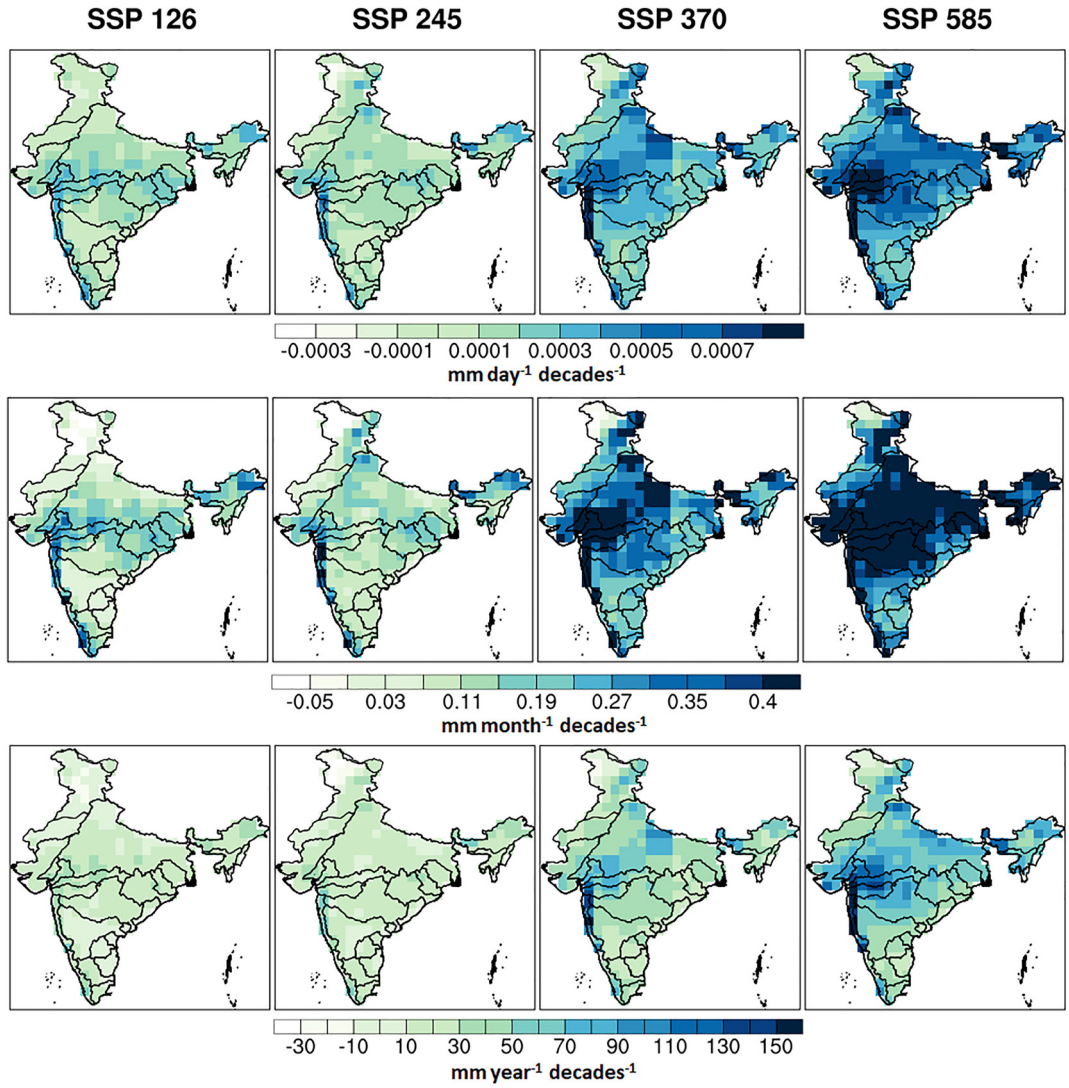

Figure 4. Daily, monthly and yearly precipitation trend per decade from 2021 to 2100 for low to high emission scenarios.

precipitation from SSP1-2.6 to SSP5-8.5 emission scenarios over the different IRBs. The spatial extension of the projected absolute mean precipitation expends over the lower Ganga river basin for 100–150 mm/day in the SSP5-8.5; also Indus River basin was found to be very deficient in mean precipitation, approximately 0–100 mm/day. We found that the West flowing Tapti to Tadri and Bharamputra river basins are projected to increase precipitation (200–500 mm/day), which leads to more flood conditions over the basin catchment area. And this will affect the estimated projected population during 2050 (CWC, 2021), approximately 106.67 million over these river basins (Table S1 in Supporting Information S1). Although, based on low to high emissions, the different SSPs scenarios have future challenges to adaptation and mitigation (Fan et al., 2021). In Figure 4, we found that the central IRBs, including Narmada, Tapti, Mahi, and west-flowing river basins, experienced a significant ($p < 0.05$) increasing trend of precipitation per decade, approximately 0.5×10^{-2} to 0.7×10^{-2} mm/day. Moreover, the monthly is 0.35–0.4 mm/month/decade, and annually it shows 10–30 mm/year/decade in low emission scenarios SSP1-2.6, while central western ghats areas with significant ($p < 0.05$) change (high model agreement) resulted in 150 mm/year/decade in the high emission scenarios SSP5-8.5 (Figure 4; Figure S3 in Supporting Information S1). The differences among SSPs are more distinct at the monthly scale due to variations in human activities, such as energy consumption and agricultural practices, which influence greenhouse gas emissions and land use changes. Monthly data captures these variations, resulting in diverse climate patterns among SSPs. In contrast, the daily scale is influenced by shorter-term weather variability and localized weather systems, masking the underlying differences among SSPs.

10.1029/2023EF003556

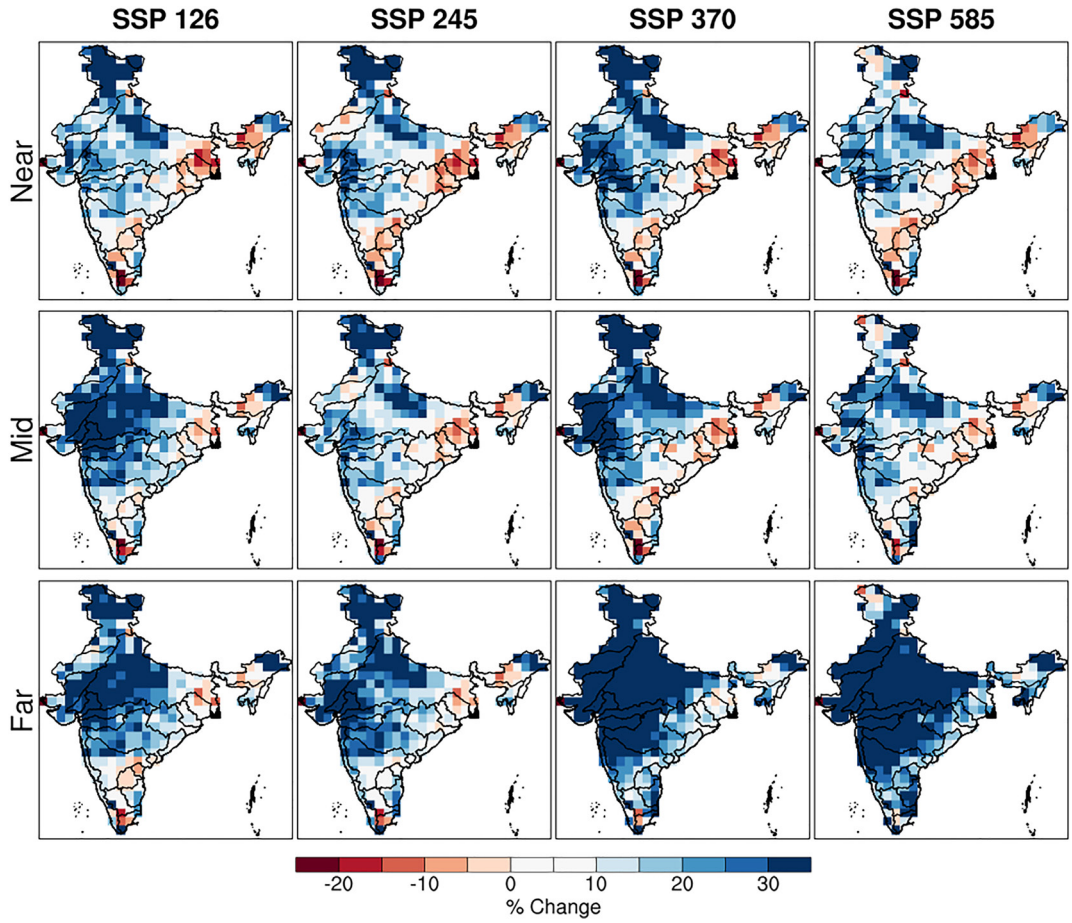

Figure 5. Annual mean precipitation change (%) for Near- (2021–2040), Mid- (2041–2060), and Far-future (2081–2100) relative to 1995–2014.

Next, we explore the projected changes in precipitation during the near, mid, and far future with the reference period 1995–2014, plotted in Figure 5 and significant test result in Figure S4 in Supporting Information S1. In the near future, the upper Ganga and Indus river basin found to be 10–30 mm/day change in precipitation, at the increasing temperature very likely to range from 1.3 to 1.9°C under the very high GHG emissions scenario (SSP5-8.5) (IPCC, 2021). However, in the far future western parts of the IRBs projected about 0–30 mm/day changes in precipitation in low emission scenarios SSP1-2.6 and SSP2-4.5 under the increasing temperature very likely 1.3–3.5°C during 2081–2100. The projected daily precipitation is highly concentrated over the western and central IRBs. This may be due to the moisture flux wind circulations over the Arabian and Indian Ocean dipole, primarily controlling changes in precipitation over the Indian continent (Rodwell & Hoskins, 2001). India's eastern ghats river basins were found to be decreased (0% to −20%) in daily precipitation; however, in the far future, it will increase (0%–15%). These areas have significant change but low model agreement at 95% significance level. And the previous researcher found that due to increase in air temperature over the Indian continent, predominantly north western part of India and it's may enhance the possibility of an increased moisture-holding capacity of the atmosphere, resulting in extremity in precipitation over north-west India (Mishra et al., 2020; Sarkar & Maity, 2022). Another analysis by Suman and Maity (2020) resulted in an increment of the extremes over the southern part due to the moisture flux deviation during the monsoon season, which strengthened eastward moisture flux over the Indian continent. Here, we found high variability in precipitation from low (SSP1-2.6) to high (SSP5-8.5) emission scenarios. Most of India's western river basins are projected to increase daily precipitation near to far future. In the mid-future, only SSP1-2.6 and SSP3-7.0 show a significant increasing change (high model agreement) of about 30% precipitation per day over the West flowing River Kutch & Saurashtra including Luni, Indus, and Upper Ganga River Basins. And these changes lead to low (SSP1-2.6) and high (SSP3-7.0) challenges to adaptation and mitigation in the future.

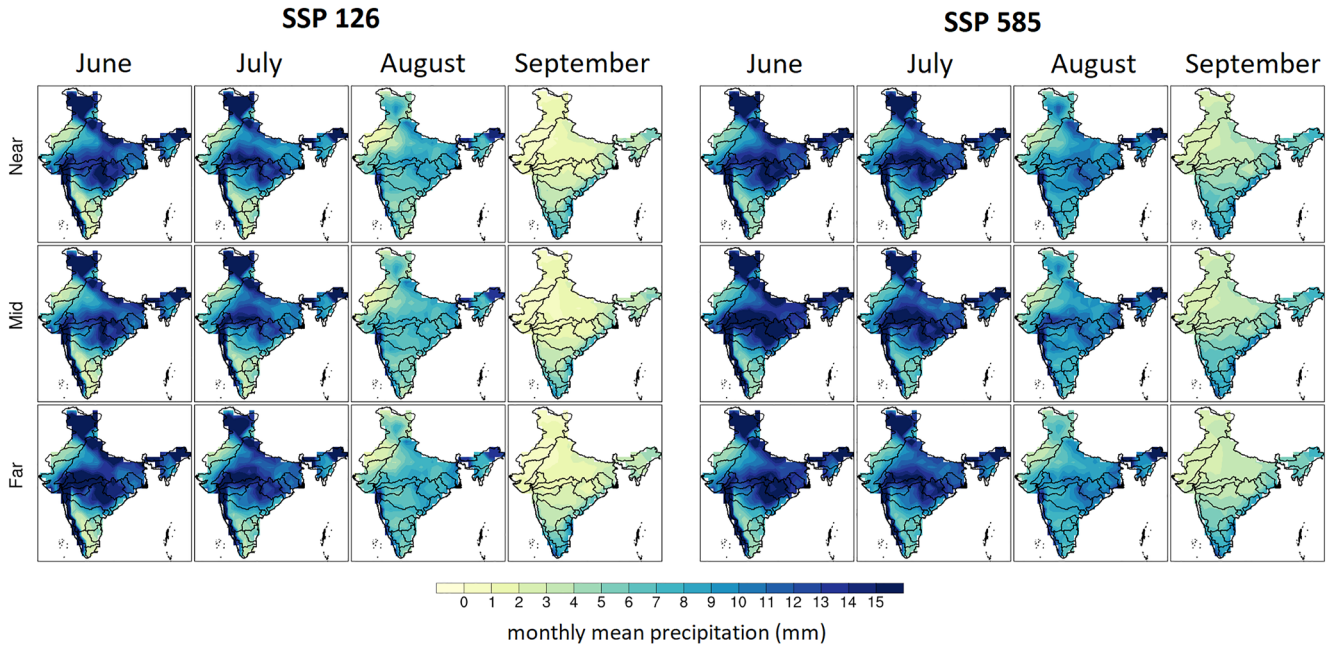

Figure 6. Monthly mean precipitation climatology for monsoon season over the IRBs at low (SSP1-2.6) and high (SSP5-8.5) emission scenarios.

Figure 6 shows the spatial distribution of the climatological mean precipitation for the months JJAS (June-July-August-September). We found that the mean precipitation climatology varies from 12 to 15 mm/day, highly focused over central India, the Western Ghats, Indus, and Brahmaputra River Basins during the June and July months in both the low (SSP1-2.6) and high (SSP5-8.5). While Inland drainage of Rajasthan, Krishna, Cauvery, and Pennar river basins are found to have moderate mean precipitation of 4–7 mm/day. The lower Ganga river basin is found to be a decrease in monthly mean precipitation of approximately 7–11 mm/day in the near future. This resembles droughts over the basin reported (CRED, 2021) during the JJAS period of 2002 and 2015, affecting about 300 million people in India. And this may project the flash drought intensification due to enhanced land-atmospheric and inter-annual climate variability due to El Nino Southern Oscillation (ENSO) (Mahto & Mishra, 2023; Mishra et al., 2021). Also, a recent study based on historical data sets resulted in the high surface pressure over the Tibet region, which initiated a decline rate in circulation intensity of the mid-tropospheric cyclone that reveals low precipitation (Singh et al., 2022). This decrease in rainfall and extreme temperature increase will affect the sugarcane crop's sugar content (Table S1 in Supporting Information S1) which is the major crop of the Ganga river Basin.

However, in August, monthly mean precipitation climatology over the IRBs, is approximately 5–10 mm/day, while inland drainage of Rajasthan shows deficient precipitation of about 3 mm/day. Despite that, in the September south-peninsular IRBs Cauvery, the East-flowing River (EFR) between Mahanadi and Kanyakumari projected mean precipitation from 4 to 9 mm/day. This may lead to the urban flood over Hyderabad, Bengaluru, and Chennai, like Indian cities situated under the peninsular IRBs. And the finding is consistent with the previous research (Suman & Maity, 2020), which concluded that in the JJAS months, the moisture-weighed wind deviates from the Arabian Sea toward the Indian continent, which reveals more intensified moisture flux that causes more precipitation extreme events over WRF-TT and central India. According to the global disaster report (CRED, 2021) on extreme events, during JJAS months in India, about 1,282 lives were claimed due to deadly floods. This variability in the Indian monsoon under different projected warming scenarios of CMIP6 was found to increase due to global mean temperature (Katzenberger et al., 2021).

3.3. Changes in Extreme Precipitation

Next, we analyze the intensity of the precipitation extremes (magnitude of precipitations extremes per unit time) at 5-day total precipitation, consecutive dry and wet days for observed, as well as historical and projected climate models for new SSPs scenarios (Figure 7). Here we found that, in the last 71 years, from 1951 to 2021, IRBs

10.1029/2023EF003556

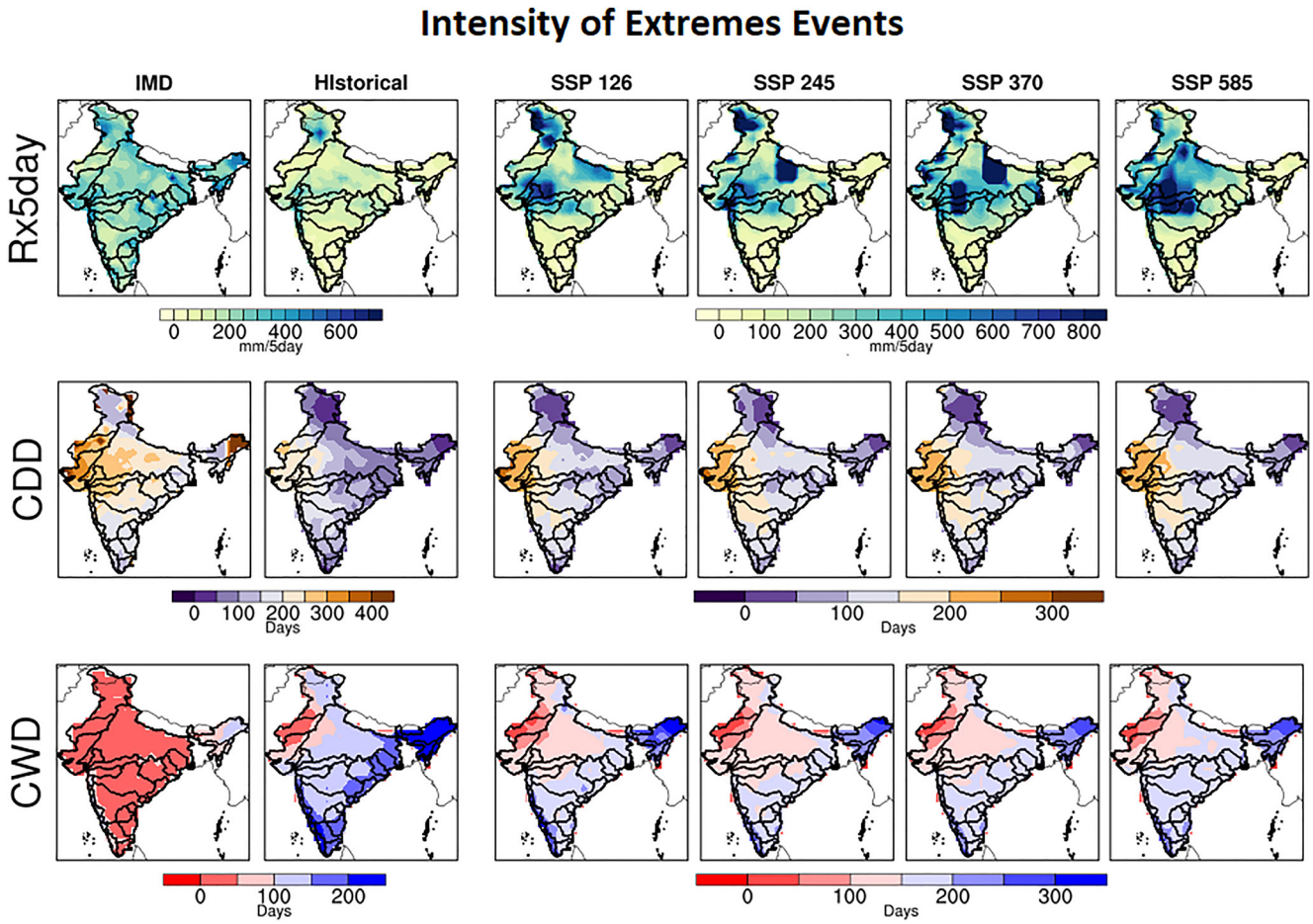

Figure 7. Spatial changes in the intensity of extreme precipitation events from observed (1951–2021), historical (1951–2014), and projected (2021–2100) for all SSP scenarios.

experienced a high intensity of 5-day total rainfall of approximately 300–500 mm over the western Ghats and central IRBs. Despite that, the projected 5-day total precipitation shows the highest value of precipitation of 600–900 mm over the Indus, western Ghats, upper Ganga basin, and central IRBs, including Narmada, Mahi, and Tapti. The intensity of 14.28% was found to be increased under SSP2-4.5 over the upper Ganga and Indus river basins. Also, this was previously reported that the Ganga River Basin faced normal to severe flood events during the 2019 flood season (CWC, 2021). The maximum intensity of dry days is found over the Inland drainage of Rajasthan, West-flowing river basin Tapti to Tadri. Moreover, the projected dry days increased by about 100–150 days/86 years. On the other hand, during the period 1951–2021, observed rainfall shows the intensity of wet days increases approximately 100–250 days/71 years over the Brahmaputra and Barak and Other, eastern and western ghats river basins, including Mahanadi, Brahmani, Subarnarekha over the IRBs. However, the projected wet days are increased in similar basins, including Indus and Upper Ganga basins, by approximately 150–350 days/86 years. Also over the northeast river basins and western ghats, the mean rainfall ranges from 8 to 16 mm per day, and there is a corresponding higher intensity (150–300 days) of consecutive wet days in these regions. And according to Zhao and Dai (2022) as the climate warms, there is a tendency for the atmosphere to hold more moisture, resulting in an increase in both mean rainfall and extreme rainfall events. Based on low to high emissions and human-made anthropogenic land use, the different SSPs scenarios established by climate scientists for integrated research on future climate change and its impacts, vulnerability, adaptation, and mitigation (Fan et al., 2021).

Figure 8 represents the spatial changes in the frequency of extreme events in the last 71 years and the projected 86 years in different emission scenarios. The number of 5-day of heavy precipitation events is approximately 300–400 over the Indus, central India Narmada, Godavari, and Mahanadi River basins. And the frequency of

10.1029/2023EF003556

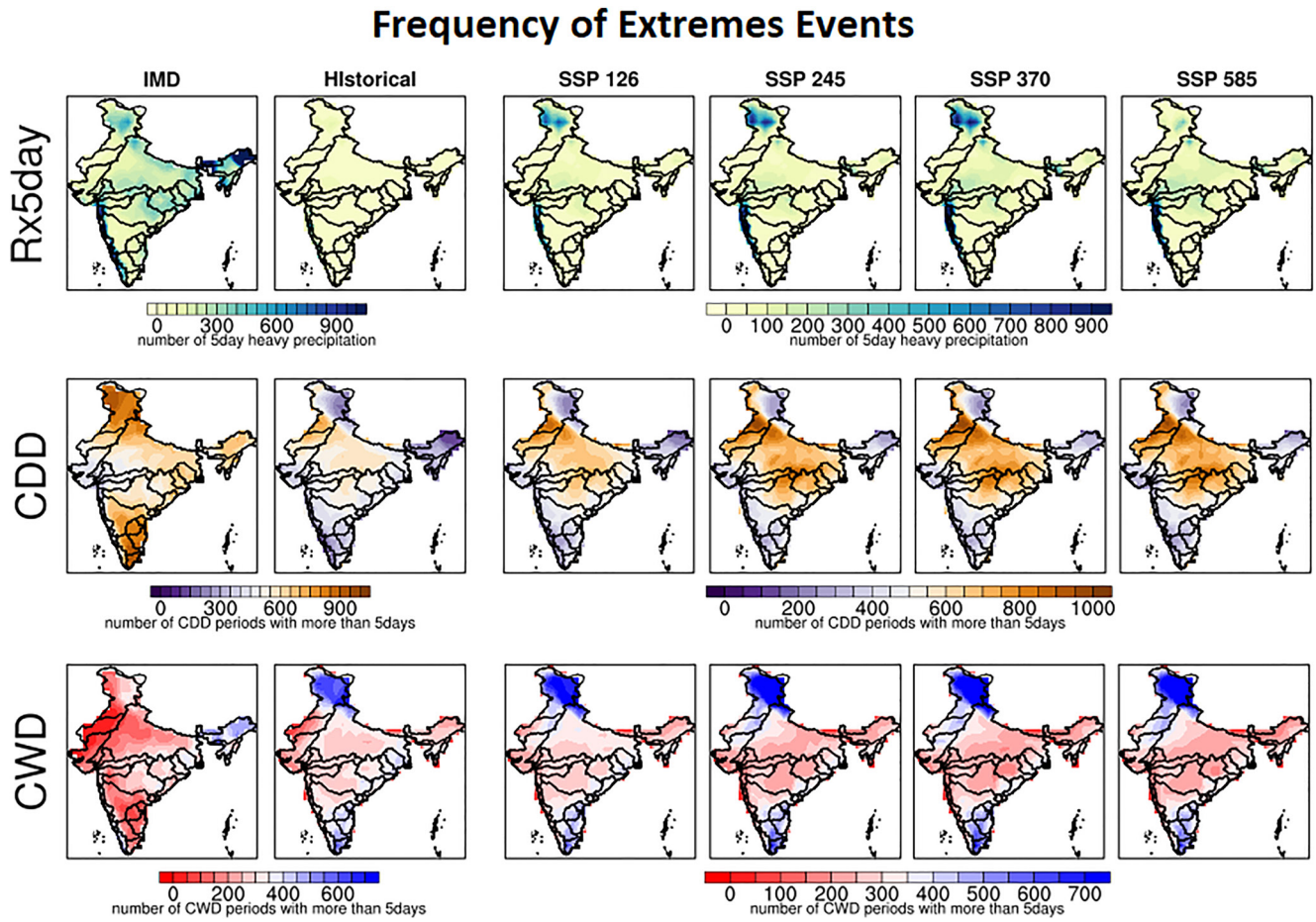

Figure 8. Spatial changes in the frequency of extreme precipitation events from observed (1951–2021), historical (1951–2014), and projected (2021–2100) for all SSP scenarios.

5-day heavy rainfall is mostly dominated over the Brahmaputra and west-flowing river basins from Tapti to Kanyakumari River basins from 1951 to 2014, with approximately 600–900 events. Moreover, the projected maximum number of 5-day of heavy precipitation events is approximately 700–1000, mainly concentrated over the Indus and Western Ghats. And this type of 5-day heavy precipitation leads to flash floods over the downstream situated cities in the Indus river basins and urban floods in western ghats and megacities like Mumbai and Pune. And the finding is consistent with those (Saha & Sateesh, 2022). The projected frequency of consecutive dry days (i.e., number of CDD more than 5-day) was found to increase (600–800 events) in the middle to lower Ganga basins, Mahanadi, lower Indus basin, Brahmani, and Subarnarekha. And during far-future periods, the frequency would be more prominent than intensity in the strong forcing scenarios like SSP5-8.5 (Sarkar & Maity, 2022). However, the projected frequency of consecutive wet days (i.e., number of CWD more than 5-day) resulted in approximately 350–700 days over the Upper Ganga basin, inland drainage of Rajasthan, Cauvery, and East flowing river basin Mahanadi to Kanyakumari. And this depicts that the projected frequency of rainfall extremes has increased over the western Ghats, Indus River basin, and northeast river basins, including Brahmaputra and Barak and other river basins. Previous researchers found a significant change in extremes using CMIP6 over India due to global warming levels (Gusain et al., 2020).

Further, we investigate the changes in the intensity of the precipitation extremes in the Near, Mid, and Far future (Figure 9). The intensity of the extremes is found to be increased in the far and middle future as a comparison to the middle and near future, respectively. The intensity of the 5-day total rainfall will increase in the central and western river basins in the near future, while in the mid and far future, the intensity of 5-day precipitation has shifted over the upper Ganga basin. Moreover, in the far future high emission scenarios SSP5-5.8, the intensity of precipitation extremes high concentrations approximates 500–700 mm/5-day over the central IRB, including

10.1029/2023EF003556

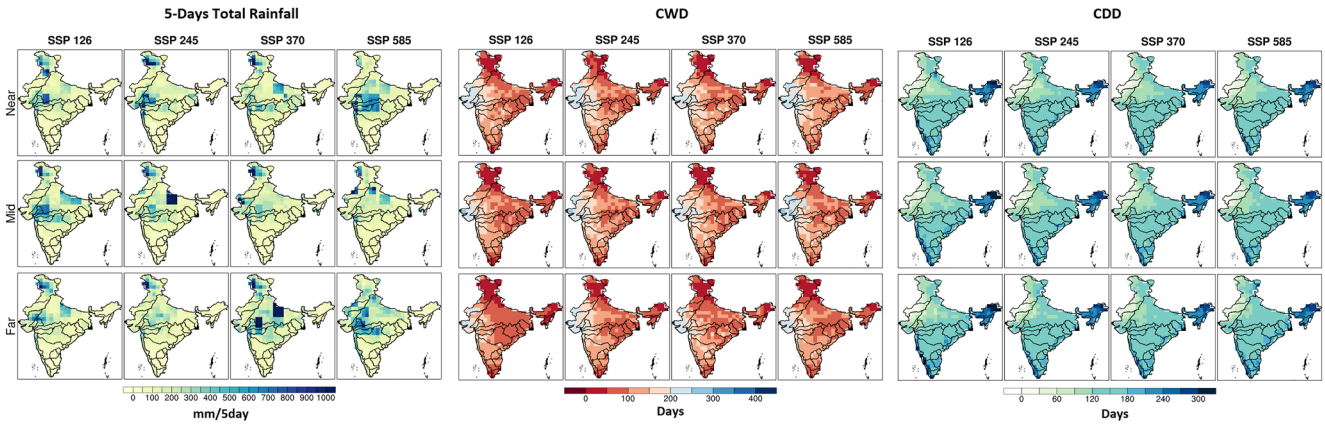

Figure 9. Near, mid, and far future changes in precipitation extremes for day's total 5-day rainfall, Consecutive wet days (CWD), and consecutive dry days (CDD) over all the SSPs.

Narmada, Mahi, Tapti, inland drainage Rajasthan and western part of the Ganga basin. Indian summer monsoon rainfall (ISMR) mainly controls these changes in precipitation by the circulation of wind-based moisture transport. The intensity of the wet day's increases from low to high emission scenarios over the west-flowing river basins. Kulkarni et al. (2020) state that the convergence of moisture flux from the Arabian Sea to central India is the leading cause of extreme rainfall's enchantment over the central IRBs like Narmada, WFR-TT, etc. And we conjecture that due to this flux convergence and projected precipitation in different scenarios during the near future, Indian western and central river basins might cause precipitation extremes. This indicates that future challenges are high for mitigation and low for adaptation with SSP5-8.5 (Fan et al., 2021). This future challenge needs to be the development of watershed management. A previous study revealed that Rainwater Harvesting (RWH) could be an innovative and sustainable environmental solution to mitigate flood hazards (Tamagnone et al., 2020).

Next, we estimate the heavy (at 90th percentile) to very heavy (at 95th percentile) precipitation extremes in the near, mid, and far future in Figure 10. And we found that the intensity of the heavy precipitation at the 90th percentile has increased in the low emission scenarios, approximately 4%–10% in the western part of India in the near and mid future, while in the far future, it only concentrated over the inland drainage of Rajasthan and West flowing river basin. On the other hand, heavy precipitation (90th percentile) varies from 3% to 7% over the Middle Ganga, Narmada, Godavari, and Mahanadi River Basins in the higher emission scenarios. Similarly, the very heavy precipitation at the 95th percentile results show a similar pattern but with low intensity, approximately 2%–5% very heavy precipitation. The intensity of the very heavy precipitation increases over the central IRBs from 1% to 4%, with increasing emission scenarios from SSP2-4.5 to SSP5-8.5. Indeed, the dynamic part of the different SSPs scenarios is to represent the projected changes in hydroclimate extremes with their probable uncertainties (Fan et al., 2021). Moreover, the frequency of the heavy to very heavy precipitation at the 90th and 95th percentile, respectively, increased in the near to far future over the Brahmaputra and west-flowing Tapti to Tadri river basins (Figure 11). Also, earlier research reported that increasing precipitation extremes are mainly caused by dynamic and local thermodynamics, which have more moist static energy (Saha & Sateesh, 2022). And this will lead to increases in low-level convergence over eastern, central, and western flowing IRBs during the 21st century.

In Figure 12, the probability of the precipitation extremes is found to be increased in the central IRBs, including the central Ganga basin, Narmada, Sabarmati, Mahi, and northwest part of the Godavari basin, with approximately 100–500 mm/day return level. To depict, the probability of occurrence of precipitation extremes increases with the high emission scenarios in the 21st century from 2021 to 2100. The highest probability of precipitation extremes was found in the upper Ganga and Indus River basins at 500–1,000 mm/day return levels. Moreover, the high emission scenarios SSP3-7.0 shows a 900–1,000 mm/day return level over the west-flowing Kutch to Luni River basin and widespread over the central India river basins. In northwestern India, the disappearance of the signal under SSP5-8.5 can be attributed to increased warming and changes in atmospheric circulation patterns, resulting in a different pattern of precipitation distribution compared to SSP1-2.6 to SSP3-7.0. It may due to

10.1029/2023EF003556

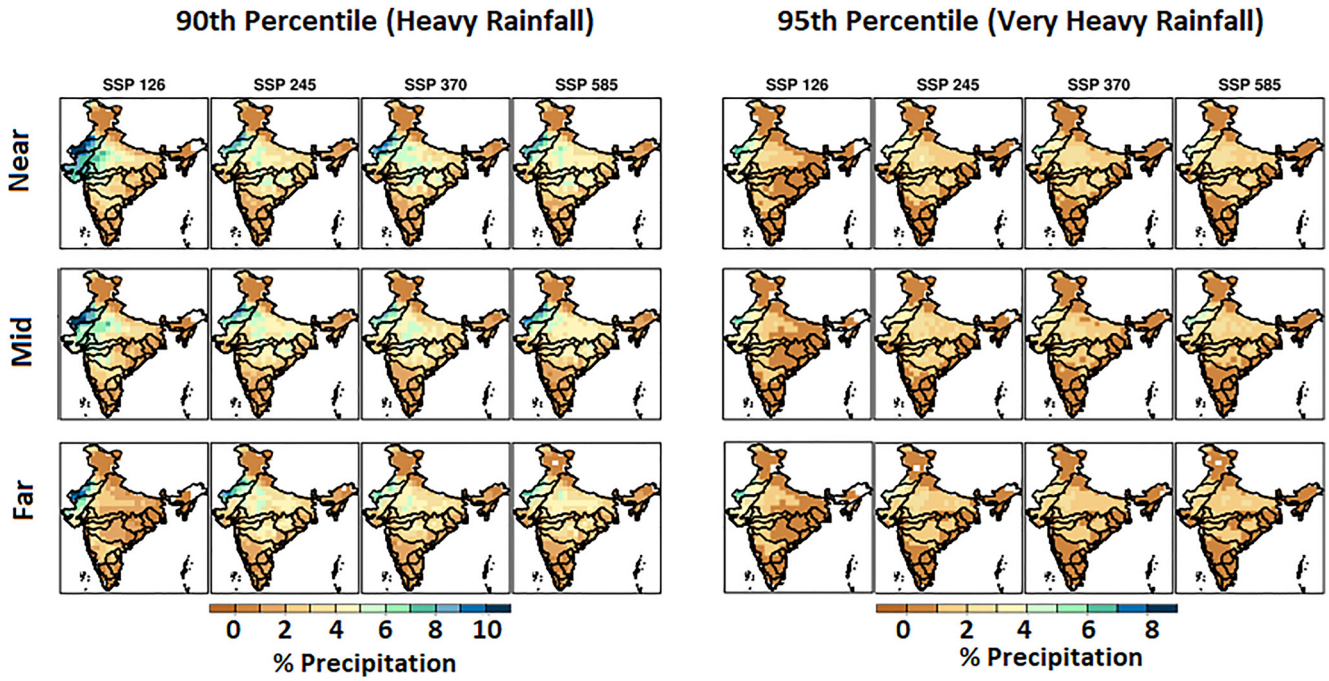

Figure 10. Heavy (90th percentile) to Very heavy (95th percentile) percentage precipitation changes in near, mid, and far future.

the high greenhouse gas emissions and limited climate mitigation efforts, leading to significant warming of the climate system under SSP5-8.5. The estimated return level helps examine the extreme precipitation, leading to a derived Probable Maximum Flood (PMF), and it will be used to design high-risk infrastructures such as large dams and nuclear power plants where failure would be catastrophic (Visser et al., 2022).

Figure 13 decipher the changes in hydroclimate extremes from dryness to wetness in the near, mid, and far future. Moreover, the decadal changes in observed dryness and wetness are shown in Figure S5 in Supporting Information S1. The IRBs show changes in wet to dry conditions, in which western river basins (Surplus, $0 \leq SPI \leq +2$), while northern east river basins (Deficit, $-1.5 \leq SPI \leq 0$) in the last 71 years from 1951 to 2021 (Figure 13).

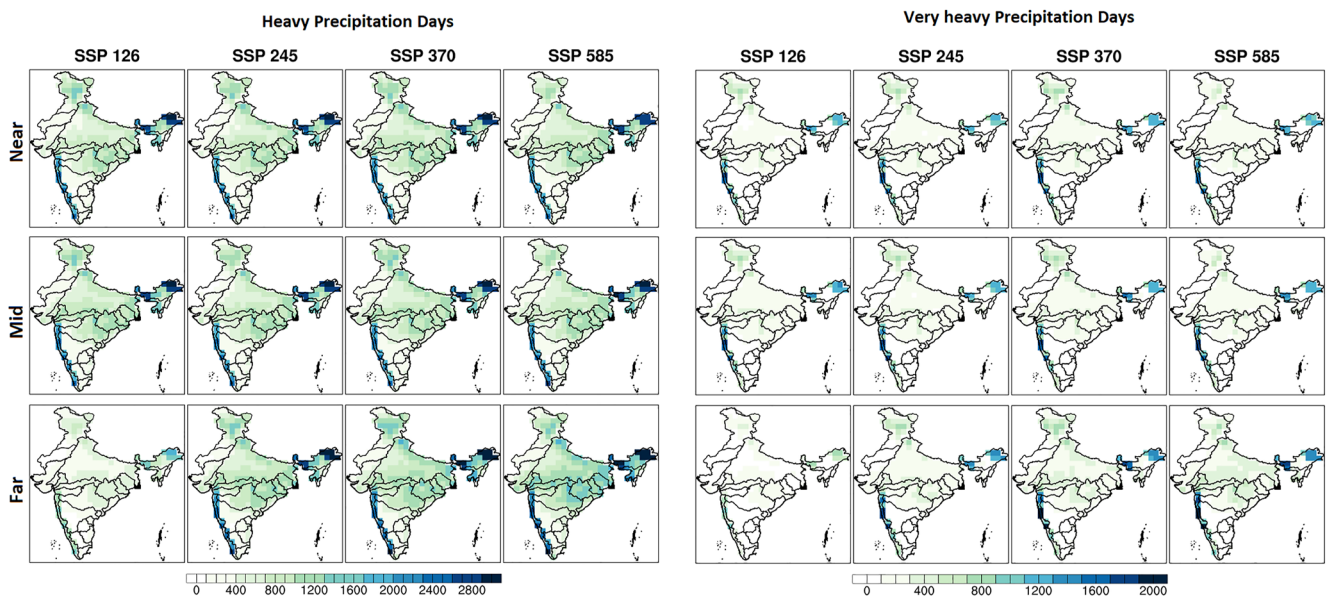

Figure 11. Number of Heavy (90th percentile) to Very Heavy (95th percentile) precipitation days over the IRBs.

10.1029/2023EF003556

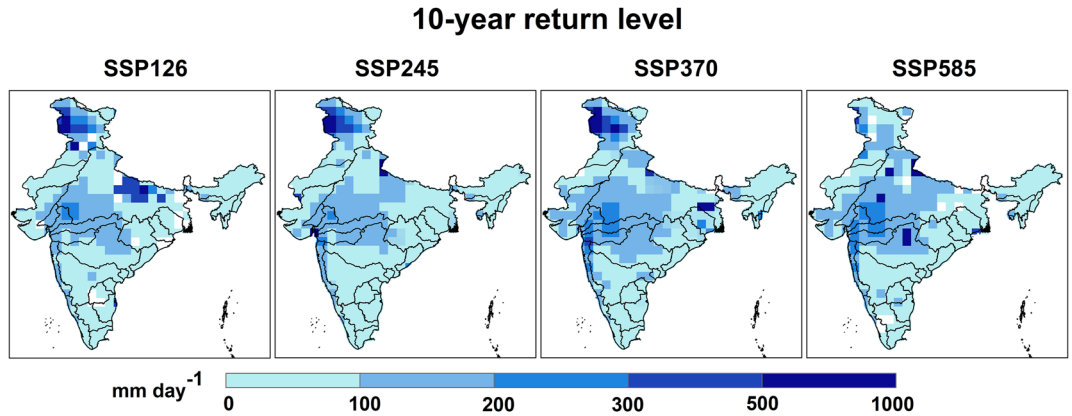

Figure 12. Spatial estimation of return level of precipitation extremes over the Indian river basins (IRBs) at 10-year return levels (10%, probability storms), using 2021–2100 projected SSP scenarios. The white color represents the unprocessed data sets.

And this is consistent with previous findings that showed an increasing and shifting pattern of precipitation over the IRBs during the post-1980 (Chaubey et al., 2022; Sarkar & Maity, 2022). Also, this decline in rainfall over northeast India is consistent with previous researchers (Kuttippurath et al., 2021), which conclude that its due to the changes in land cover and become detrimental to vegetation activity.

Moreover, the near future IRBs show widespread annual drought conditions in most of the northwestern part of the IRBs as $-2.5 \leq SPI \leq +2$ in SSP2-4.5 and SSP5-8.5. During the near future, the spatial changes of an extreme dry spell over the IRBs show staggered nature for SPI (presence of pixels with increases in the frequency of dry wet spells). The frequency of dry spells over India is projected to increase, which may be amplified with time and radiative forcing (Salvi & Ghosh, 2016). Also, previous research concluded that under the low to high emission

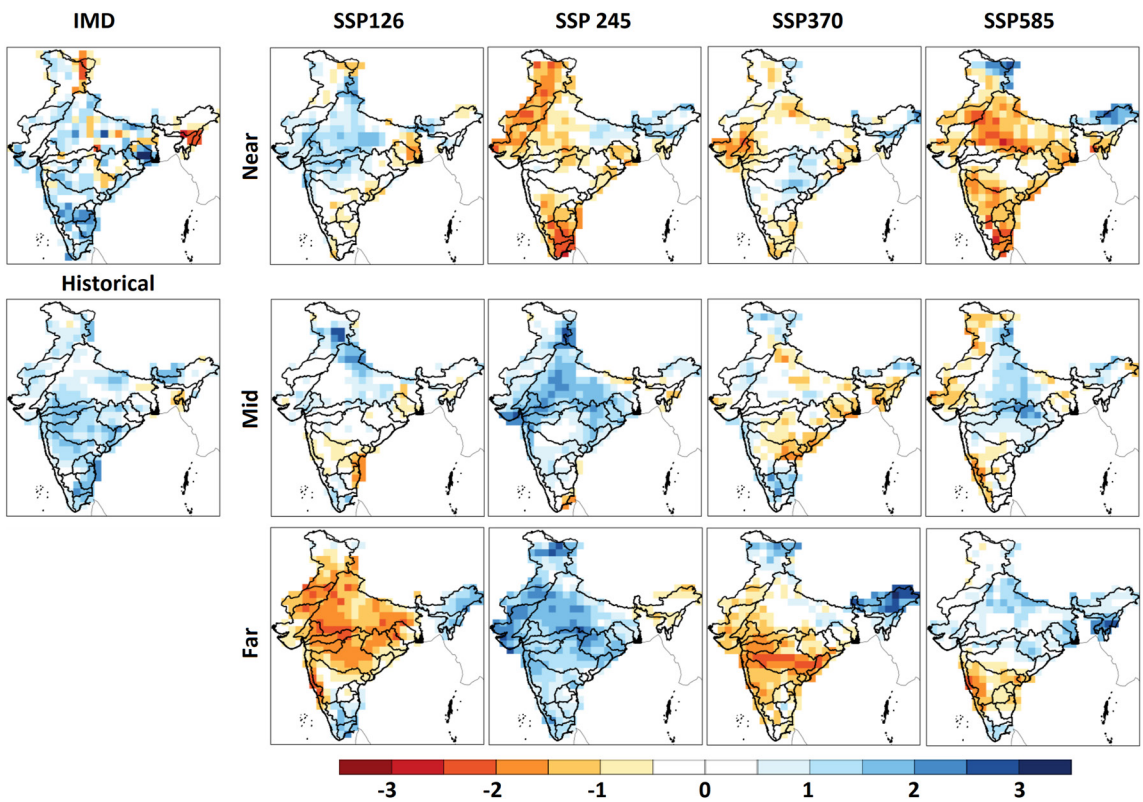

Figure 13. Changes in average intensity of estimated wet to dry stage at a monthly time spanning over the Indian river basins.

scenario Ganga river basin, central and north-west river basin, and peninsular IRBs showed more frequent occurrences of a moderate and severe dry spells (Mujumdar et al., 2020; Salvi & Ghosh, 2016). The CWC (2021) reported that the estimated population would be increased (8.06%) over the Ganga River Basin, and the per capita average water availability (cum) would be decreased by 8.11% from 2025 to 2050. However, the mid-future IRBs would face the normal to wet condition $-1 \leq \text{SPI} \leq +2.5$. It illustrates the SSPs variations increased in the near to mid-future may be attributed to inter-model differences in simulating the surface temperature (Sarkar & Maity, 2022). The far future IRBs are estimated to have very high wetness conditions $0 \leq \text{SPI} \leq +3$. The SPI resulted that MMM projected a weak declining trend all the time series for the post-2070 by the high emission scenario compared to the medium emission scenario (Mujumdar et al., 2020). This depicts the precipitation extremes will increase over the IRBs in the far future (2081–2100), with increasing global temperature very likely 1.8–5.7°C (IPCC, 2021). These variations in dryness to wetness in different SSPs scenarios play a vital role in identifying the future aspects of hydroclimate extremes with their possible uncertainties (Riahi et al., 2017).

3.4. Uncertainty Due To Different Climate Scenarios

The simulated outputs of the different CMIP6 model have high uncertainty in extremes; however, bias correction help to reduce the uncertainty in extremes. Many previous researchers used the multi-model mean (MMM) approach to reduce the uncertainty in projected extremes (Katzenberger Et Al., 2021). However, in our study MMM approach has been used, which shows uncertainty in daily rainfall from −0.3 to 0.9. The spatial changes in mean areal precipitation show drastic changes in SSP3-7.0, that is, 1.83 mm/day mean precipitation, which is higher than the high emission scenarios SSP5-8.5, which may have the uncertainty in areal mean precipitation over the different IRBs. The SSP2-4.5 shows uncertainty over west-flowing river basins during the mid-future, about 10%–15% of decrement annual mean precipitation compared with low emission SSP1-2.6. Moreover, in SSP5-8.5 scenarios, there is a decrement in the frequency of extreme precipitation over the Indus River basin compared with other low-emission scenarios. Thus for the reliability of the extreme precipitation over the regional river basin, more appropriate bias correction should be used for different climate scenarios, which will be helpful to reduce this uncertainty (O'Neill et al., 2020; Riahi et al., 2017).

4. Conclusion

In many IRBs extreme rainfall are projected to increase and intensify throughout the 21st century, with greater increases after the 2040s. They are projected to reach unprecedented levels by the end of the century in the absence of strong mitigation measures, such as achieving the Paris Agreement targets to limit global warming to between 1.5 and 2.0°C. The frequency of precipitation extremes over the west-flowing river basins and western Ghats of India is going to increase during the near and mid future, while intensity will be dominated over the Indus and upper Ganga basins. The daily mean average rainfall is projected to increase with low to high emission scenarios. Due to intensification of extreme rainfall, western ghats, Indus, West, and central IRBs will be highly vulnerable. Moreover, major cities like Mumbai and Pune, situated in the west-flowing river basins would have a high potential for urban flooding due to the increasing future precipitation extremes. In the near future, the June-July months of the monsoon season will see heavy rainfall with high intensity over the western and central IRBs. Moreover, during September in the monsoon season, the peninsular IRBs will experience heavy rainfall leading to increased risk of urban flooding in highly populated cities like Hyderabad, Bengaluru, and Chennai. Over the different IRBs, the simulated output of CMIP6 depicted a high rate of change in hydroclimate extremes in all climate scenarios except SSP1.26, which signifies the current possible scenario for the extremes. The regional study reliability is also challengeable due to uncertainty between the models output and its coarser resolution. The extreme pattern observed under SSP1-2.6 to SSP3-7.0 suggests low to high challenges to mitigation and adaptation strategies, but that may not be as prominent or consistent under the high-emission scenario of SSP5-8.5 over different IRBs. The effects of climate change under SSP5-8.5 may still lead to significant impacts and changes in precipitation patterns, and this study suggests that to develop long-term adaptation and mitigation strategies to reduce the hydroclimate vulnerability over the major IRBs.

Finally, the significant changes in the frequency of hydro-climate extreme events may have a considerable impact on agriculture, heaths, and other socio-economic conditions of the society. The findings presented here are supporting basin-wise climate adaptation and mitigation strategies, including water and emergency services policies to minimize risk due to extremes in the basins.

Conflict of Interest

The authors declare no conflicts of interest relevant to this study.

Data Availability Statement

The observed and CMIP6 data sets (Observed Rainfall And CMIP6 Data (Version 1.0.0); Chaubey and Mall (2023a)) were obtained from India Meteorology Department (IMD) (URL: https://www.imdpune.gov.in/lrfindex.php) and Earth System Grid Federation (URL: https://esgf-node.llnl.gov/search/cmip6/) respectively. The software (Precipitation Trend and Bias Correction: 15 Jul 2023 Release (Version 1.0.0)) on which this article is based are available in Chaubey and Mall (2023b).

Acknowledgments
The authors acknowledge the DST-Mahamana Centre of Excellence in Climate Change Research; funding for this study is gratefully recognized as being provided by the Department of Science and Technology through projects under Climate Change Programme, Department of Science and Technology, New Delhi, for financial support (DST/CCP/CoE/80/2017(G)).

References

Anand, V., & Oinam, B. (2020). Future land use land cover prediction with special emphasis on urbanization and wetlands. *Remote Sensing Letters*, *11*(3), 225–234. https://doi.org/10.1080/2150704X.2019.1704304

Bothale, R. V., & Katpatal, Y. B. (2016). Trends and anomalies in extreme climate indices and influence of El Niño and La Niña over Pranhita catchment in Godavari basin, India. *Journal of Hydrologic Engineering*, *21*(2), 05015023. https://doi.org/10.1061/(asce)he.1943-5584.0001283

Cannon, A. J., Sobie, S. R., & Murdock, T. Q. (2015). Bias correction of GCM precipitation by quantile mapping: How well do methods preserve changes in quantiles and extremes? *Journal of Climate*, *28*(17), 6938–6959. https://doi.org/10.1175/JCLI-D-14-00754.1

Chaubey, P. K., & Mall, R. K. (2023a). Observed rainfall and CMIP6 data (version 1) [Dataset]. Zenodo. https://doi.org/10.5281/zenodo.8151782

Chaubey, P. K., & Mall, R. K. (2023b). Precipitation Trend and bias correction: Jul 15, 2023 release (version 1) [Software]. Zenodo. https://doi.org/10.5281/zenodo.8151900

Chaubey, P. K., Mall, R. K., Jaiswal, R., & Payra, S. (2022). Spatio-temporal changes in extreme rainfall events over different Indian river basins. *Earth and Space Science*, *9*(3), 1–21. https://doi.org/10.1029/2021EA001930

CRED. (2021). *Disasters in numbers. Extreme events defining our lives Executive summary*. Centre for Research on the Epidemiology of Disasters. Retrieved from https://cred.be/sites/default/files/2021_EMDAT_report.pdf

CWC. (2021). *Water and related statistics*. Central Water Commission (CWC), Government of India, Information System Organisation. Retrieved from http://www.cwc.gov.in/sites/default/files/water-and-related-statistics-2021compressed-2.pdf

Douglas, I. (2009). Climate change, flooding and food security in south Asia. *Food Security*, *1*(2), 127–136. https://doi.org/10.1007/s12571-009-0015-1

Fan, X., Miao, C., Duan, Q., Shen, C., & Wu, Y. (2021). Future climate change hotspots under different 21st century warming scenarios. *Earth's Future*, *9*(6). https://doi.org/10.1029/2021EF002027

Gadgil, S., & Gadgil, S. (2006). The Indian monsoon, GDP and agriculture. *Economic and Political Weekly*, *41*(25), 4887–4895.

Giorgi, F., Coppola, E., & Raffaele, F. (2018). Threatening levels of cumulative stress due to hydroclimatic extremes in the 21st century. *Npj Climate and Atmospheric Science*, *1*(1), 18. https://doi.org/10.1038/s41612-018-0028-6

Goswami, B. N., Venugopal, V., Sangupta, D., Madhusoodanan, M. S., & Xavier, P. K. (2006). Increasing trend of extreme rain events over India in a warming environment. *Science*, *314*(5804), 1442–1445. https://doi.org/10.1126/science.1132027

Guhathakurta, P., Sreejith, O. P., & Menon, P. A. (2011). Impact of climate change on extreme rainfall events and flood risk in India. *Journal of Earth System Science*, *120*(3), 359–373. https://doi.org/10.1007/s12040-011-0082-5

Gupta, V., & Jain, M. K. (2018). Investigation of multi-model spatiotemporal mesoscale drought projections over India under climate change scenario. *Journal of Hydrology*, *567*, 489–509. https://doi.org/10.1016/j.jhydrol.2018.10.012

Gupta, V., Singh, V., & Jain, M. K. (2020). Assessment of precipitation extremes in India during the 21st century under SSP1-1.9 mitigation scenarios of CMIP6 GCMs. *Journal of Hydrology*, *590*, 125422. https://doi.org/10.1016/j.jhydrol.2020.125422

Gusain, A., Ghosh, S., & Karmakar, S. (2020). Added value of CMIP6 over CMIP5 models in simulating Indian summer monsoon rainfall. *Atmospheric Research*, *232*, 104680. https://doi.org/10.1016/j.atmosres.2019.104680

Huang, H., Cui, H., & Ge, Q. (2021). Assessment of potential risks induced by increasing extreme precipitation under climate change. *Natural Hazards*, *108*(2), 2059–2079. https://doi.org/10.1007/s11069-021-04768-9

IPCC. (2021). In *Climate change 2021 the physical science basis summary for policymakers working group I contribution to the sixth assessment report of the intergovernmental panel on climate change*.

Jaiswal, R., Mall, R. K., Singh, N., Lakshmi Kumar, T. V., & Niyogi, D. (2022). Evaluation of bias correction methods for regional climate models: Downscaled rainfall analysis over diverse agroclimatic zones of India. *Earth and Space Science*, *9*(2). https://doi.org/10.1029/2021EA001981

John, A., Douville, H., Ribes, A., & Yiou, P. (2022). Quantifying CMIP6 model uncertainties in extreme precipitation projections. *Weather and Climate Extremes*, *36*(February), 100435. https://doi.org/10.1016/j.wace.2022.100435

Kannan, S., & Ghosh, S. (2013). A nonparametric kernel regression model for downscaling multisite daily precipitation in the Mahanadi basin. *Water Resources Research*, *49*(3), 1360–1385. https://doi.org/10.1002/wrcr.20118

Katzenberger, A., Schewe, J., Pongratz, J., & Levermann, A. (2021). Robust increase of Indian monsoon rainfall and its variability under future warming in CMIP6 models. *Earth System Dynamics*, *12*(2), 367–386. https://doi.org/10.5194/esd-12-367-2021

Kaushik, S., Rafiq, M., Joshi, P. K., Singh, T., Pandey, A. A. K. C., Dabral, P. P., et al. (2020). Hydrologic sensitivity of Indian sub-continental river basins to climate change. *Journal of Hydrology*, *12*(1), 1–15. https://doi.org/10.1016/j.gloplacha.2016.01.003

Konda, G., & Vissa, N. K. (2022). Evaluation of CMIP6 models for simulations of surplus/deficit summer monsoon conditions over India. *Climate Dynamics*, *60*(3–4), 1023–1042. https://doi.org/10.1007/s00382-022-06367-1

Krishnan, R., Sanjay, J., Gnanaseelan, C., Mujumdar, M., Kulkarni, A., & Chakraborty, S. (2020). Assessment of climate change over the Indian region: A report of the ministry of Earth sciences (MOES), government of India. In R. Krishnan, J. Sanjay, C. Gnanaseelan, M. Mujumdar, A. Kulkarni, & S. Chakraborty (Eds.), *Assessment of climate change over the Indian region: A report of the ministry of Earth sciences (MoES), Government of India*. Springer Singapore. https://doi.org/10.1007/978-981-15-4327-2

Kulkarni, A., Sabin, T. P., Chowdary, J. S., Rao, K. K., Priya, P., Gandhi, N., et al. (2020). *Precipitation changes in India. Assessment of climate change over the Indian region: A report of the Ministry of Earth sciences* (pp. 47–72). MoES), Government of India.

Kuttippurath, J., Murasingh, S., Stott, P. A., Balan Sarojini, B., Jha, M. K., Kumar, P., et al. (2021). Observed rainfall changes in the past century (1901–2019) over the wettest place on Earth. *Environmental Research Letters*, *16*(2), 024018. https://doi.org/10.1088/1748-9326/abcf78

Latif, M. (2011). Uncertainty in climate change projections. *Journal of Geochemical Exploration*, *110*(1), 1–7. https://doi.org/10.1016/j.gexplo.2010.09.011

Lenderink, G., Buishand, A., & Van Deursen, W. (2007). Estimates of future discharges of the river Rhine using two scenario methodologies: Direct versus delta approach. *Hydrology and Earth System Sciences*, *11*(3), 1145–1159. https://doi.org/10.5194/hess-11-1145-2007

Loo, Y. Y., Billa, L., & Singh, A. (2015). Effect of climate change on seasonal monsoon in Asia and its impact on the variability of monsoon rainfall in Southeast Asia. *Geoscience Frontiers*, *6*(6), 817–823. https://doi.org/10.1016/j.gsf.2014.02.009

Lutz, A. F., Immerzeel, W. W., Shrestha, A. B., & Bierkens, M. F. P. (2014). Consistent increase in high Asia's runoff due to increasing glacier melt and precipitation. *Nature Climate Change*, *4*(7), 587–592. https://doi.org/10.1038/nclimate2237

Mahto, S. S., & Mishra, V. (2023). Flash drought intensification due to enhanced land-atmospheric coupling in India. *Journal of Climate*, 1–31. https://doi.org/10.1175/JCLI-D-22-0477.1

Mall, R. K., Gupta, A., Singh, R., Singh, R. S., & Rathore, L. S. (2006). Water resources and climate change: An Indian perspective. *Current Science*, *90*(12), 1610–1626.

Mall, R. K., Srivastava, R. K., Banerjee, T., Mishra, O. P., Bhatt, D., & Sonkar, G. (2019). Disaster risk reduction including climate change adaptation over South Asia: Challenges and ways forward. *International Journal of Disaster Risk Science*, *10*(1), 14–27. https://doi.org/10.1007/s13753-018-0210-9

Mall, R. K., Chaturvedi, M., Singh, N., Bhatla, R., Singh, R. S., Gupta, A., & Niyogi, D. (2021). Evidence of asymmetric change in diurnal temperature range in recent decades over different agro-climatic zones of India. *International Journal of Climatology*, *41*(4), 2597–2610. https://doi.org/10.1002/joc.6978

Mall, R. K., Gupta, A., & Sonkar, G. (2017). Effect of climate change on agricultural crops. In *Current developments in biotechnology and bioengineering: Crop modification, nutrition, and food production* (pp. 23–46). Elsevier. https://doi.org/10.1016/B978-0-444-63661-4.00002-5

Mannshardt-Shamseldin, E. C., Smith, R. L., Sain, S. R., Mearns, L. O., & Cooley, D. (2012). Downscaling extremes: A comparison of extreme value distributions in point-source and gridded precipitation data. *Annals of Applied Statistics*, *6*(1), 484–502. https://doi.org/10.1214/09-AOAS287

Maurya, S., Srivastava, P. K., Yaduvanshi, A., Anand, A., Petropoulos, G. P., Zhuo, L., & Mall, R. K. (2021). Soil erosion in future scenario using CMIP5 models and Earth observation datasets. *Journal of Hydrology*, *594*, 125851. https://doi.org/10.1016/j.jhydrol.2020.125851

McKee (1993). The relationship of drought frequency and duration to time scales. In *Proceedings of the 8th conference on applied climatology* (Vol. 17, pp. 179–183).

McKee, T. B., Doesken, N. J., & Kleist, J. (1993). The relationship of drought frequency and duration to time scales. In *Proceedings of the 8th conference on applied climatology* (Vol. 17, pp. 179–183).

Mishra, V., Aadhar, S., & Mahto, S. S. (2021). Anthropogenic warming and intraseasonal summer monsoon variability amplify the risk of future flash droughts in India. *Npj Climate and Atmospheric Science*, *41*, 1–10. https://doi.org/10.1038/s41612-020-00158-3

Mishra, V., Bhatia, U., & Tiwari, A. D. (2020). Bias-corrected climate projections for South Asia from Coupled Model Intercomparison Project-6. *Scientific Data*, *7*(1), 1–13. https://doi.org/10.1038/s41597-020-00681-1

Mishra, V., & Lilhare, R. (2016). Hydrologic sensitivity of Indian sub-continental river basins to climate change. *Global and Planetary Change*, *139*, 78–96. https://doi.org/10.1016/j.gloplacha.2016.01.003

Mittal, N., Mishra, A., Singh, R., & Kumar, P. (2014). Assessing future changes in seasonal climatic extremes in the Ganges river basin using an ensemble of regional climate models. *Climatic Change*, *123*(2), 273–286. https://doi.org/10.1007/s10584-014-1056-9

Mujumdar, M., Bhaskar, P., Ramarao, M. V. S., Uppara, U., Goswami, M., Borgaonkar, H., et al. (2020). Droughts and floods. In R. Krishnan, J. Sanjay, C. Gnanaseelan, M. Mujumdar, A. Kulkarni, & S. Chakraborty (Eds.), *Assessment of climate change over the Indian region*. Springer. https://doi.org/10.1007/978-981-15-4327-2_6

Mukherjee, S., Aadhar, S., Stone, D., & Mishra, V. (2018). Increase in extreme precipitation events under anthropogenic warming in India. Weather and climate extremes (Vol. *20*, pp. 45–53). https://doi.org/10.1016/j.wace.2018.03.005

O'Neill, B. C., Carter, T. R., Ebi, K., Harrison, P. A., Kemp-Benedict, E., Kok, K., et al. (2020). Achievements and needs for the climate change scenario framework. *Nature Climate Change*, *10*(12), 1074–1084. https://doi.org/10.1038/s41558-020-00952-0

Pai, D. S., Sridhar, L., Rajeevan, M., Sreejith, O. P., Satbhai, N. S., & Mukhopadhyay, B. (2014). Development of a new high spatial resolution (0.25° × 0.25°) long period (1901–2010) daily gridded rainfall data set over India and its comparison with existing data sets over the region. *Mausam*, *65*(1), 1–18. https://doi.org/10.54302/mausam.v65i1.851

Rai, P., Choudhary, A., & Dimri, A. P. (2019). Future precipitation extremes over India from the CORDEX-South Asia experiments. *Theoretical and Applied Climatology*, *137*(3–4), 2961–2975. https://doi.org/10.1007/s00704-019-02784-1

Riahi, K., van Vuuren, D. P., Kriegler, E., Edmonds, J., O'Neill, B. C., Fujimori, S., et al. (2017). The shared socioeconomic pathways and their energy, land use, and greenhouse gas emissions implications: An overview. *Global Environmental Change*, *42*, 153–168. https://doi.org/10.1016/j.gloenvcha.2016.05.009

Rodwell, M. J., & Hoskins, B. J. (2001). Subtropical anticyclones and summer monsoons. *Journal of Climate*, *14*(15), 3192–3211. https://doi.org/10.1175/1520-0442(2001)014<3192:SAASM>2.0.CO;2

Roxy, M. K., Ghosh, S., Pathak, A., Athulya, R., Mujumdar, M., Murtugudde, R., et al. (2017). A threefold rise in widespread extreme rain events over central India. *Nature Communications*, *8*(1), 708. https://doi.org/10.1038/s41467-017-00744-9

Roy, S. S., & Balling, R. C. (2004). Trends in extreme daily precipitation indices in India. *International Journal of Climatology*, *24*(4), 457–466. https://doi.org/10.1002/joc.995

Saha, U., & Sateesh, M. (2022). Rainfall extremes on the rise: Observations during 1951–2020 and bias-corrected CMIP6 projections for near- and late 21st century over Indian landmass. *Journal of Hydrology*, *608*(March), 127682. https://doi.org/10.1016/j.jhydrol.2022.127682

Salehie, O., Hamed, M. M., Ismail, T. b., Tam, T. H., & Shahid, S. (2023). Selection of CMIP6 GCM with projection of climate over the Amu Darya River Basin. *Theoretical and Applied Climatology*, *151*(3–4), 1185–1203. https://doi.org/10.1007/s00704-022-04332-w

Salvi, K., & Ghosh, S. (2016). Projections of extreme dry and wet spells in the 21st century India using stationary and non-stationary standardized precipitation indices. *Climatic Change*, *139*(3–4), 667–681. https://doi.org/10.1007/s10584-016-1824-9

Sarkar, S., & Maity, R. (2022). Future characteristics of extreme precipitation indicate the dominance of frequency over intensity: A multi-model assessment from CMIP6 across India. *Journal of Geophysical Research: Atmospheres*, *127*(16), 1–22. https://doi.org/10.1029/2021JD035539

Schmidli, J., Frei, C., & Vidale, P. L. (2006). Downscaling from GCM precipitation: A benchmark for dynamical and statistical downscaling methods. *International Journal of Climatology*, *26*(5), 679–689. https://doi.org/10.1002/joc.1287

Shahi, N. K., Rai, S., Verma, S., & Bhatla, R. (2023). Assessment of future changes in high-impact precipitation events for India using CMIP6 models. *Theoretical and Applied Climatology*, *151*(1–2), 843–857. https://doi.org/10.1007/s00704-022-04309-9

Shrestha, A., Rahaman, M. M., Kalra, A., Jogineedi, R., & Maheshwari, P. (2020). Climatological drought forecasting using bias corrected CMIP6 climate data: A case study for India. *Forecasting*, *2*(2), 59–84. https://doi.org/10.3390/forecast2020004

Singh, R., Jaiswal, N., & Kishtawal, C. M. (2022). Rising surface pressure over Tibetan Plateau strengthens Indian summer monsoon rainfall over northwestern India. *Scientific Reports*, *12*(1), 1–15. https://doi.org/10.1038/s41598-022-12523-8

Sonkar, G., Singh, N., Mall, R. K., Singh, K. K., & Gupta, A. (2020). Simulating the impacts of climate change on sugarcane in diverse Agro-climatic zones of northern India using CANEGRO-Sugarcane model. *Sugar Tech*, *22*(3), 460–472. https://doi.org/10.1007/s12355-019-00787-w

Suman, M., & Maity, R. (2020). Southward shift of precipitation extremes over south Asia: Evidences from CORDEX data. *Scientific Reports*, *10*(1), 6452. https://doi.org/10.1038/s41598-020-63571-x

Tamagnone, P., Comino, E., & Rosso, M. (2020). Rainwater harvesting techniques as an adaptation strategy for flood mitigation. *Journal of Hydrology*, *586*, 124880. https://doi.org/10.1016/j.jhydrol.2020.124880

Tiwari, R., Mishra, A. K., Rai, S., & Pandey, L. K. (2023). Evaluation and projection of northeast monsoon precipitation over India under higher warming scenario: A multimodel assessment of CMIP6. *Theoretical and Applied Climatology*, *151*(1–2), 859–870. https://doi.org/10.1007/s00704-022-04299-8

Trenberth, K. E., Dai, A., Rasmussen, R. M., & Parsons, D. B. (2003). The changing character of precipitation. *Bulletin America Meteorology Social*, *84*(9), 1205–1218. https://doi.org/10.1175/BAMS-84-9-1205

Visser, J. B., Kim, S., Wasko, C., Nathan, R., & Sharma, A. (2022). The impact of climate change on operational probable maximum precipitation estimates water resources research (pp. 1–18). https://doi.org/10.1029/2022WR032247

Wang, H., Liu, F., & Dong, W. (2022). Features of climatological intraseasonal oscillation during Asian summer monsoon onset and their simulations in CMIP6 models. *Climate Dynamics*, *59*(11–12), 1–14. https://doi.org/10.1007/S00382-022-06223-2/FIGURES/12

WMO. (2017). *WMO statement on the state of the global climate in 2017 provisional release*. World Meteorological Organization. Retrieved from http://ane4bf-datap1.s3-eu-west-1.amazonaws.com/wmocms/s3fs-public/ckeditor/files/2017_provisional_statement_text_-_updated_04Nov2017_1.pdf?7rBjqhMTRJkQbvuYMNAmetvBgFeyS_vQ

Wu, H., Lei, H., Lu, W., & Liu, Z. (2022). Future changes in precipitation over the upper Yangtze River basin based on bias correction spatial downscaling of models from CMIP6. *Environmental Research Communications*, *4*(4), 045002. https://doi.org/10.1088/2515-7620/ac620e

Xu, Z., Han, Y., Tam, C. Y., Yang, Z. L., & Fu, C. (2021). Bias-corrected CMIP6 global data set for dynamical downscaling of the historical and future climate (1979–2100). *Scientific Data*, *8*(1), 1–11. https://doi.org/10.1038/s41597-021-01079-3

Zhao, T., & Dai, A. (2022). CMIP6 model-projected hydroclimatic and drought changes and their causes in the twenty-first century. *Journal of Climate*, *35*, 897–921. https://doi.org/10.1175/JCLI-D-21-0442.1